Economic Benefits for Flexible Thermostatic Loads in Multi-area HVDC-connected Power Systems

Economic Benefits for Flexible Thermostatic Loads in Multi-area HVDC-connected Power Systems

Vincenzo Trovato
Department of Electrical and Electronic Engineering
Imperial College London
London, United Kingdom

Andrea Mazza
Dipartimento Energia "Galileo Ferraris"
Politecnico di Torino
Torino, Italy

Gianfranco Chicco
Dipartimento Energia "Galileo Ferraris"
Politecnico di Torino
Torino, Italy

***Abstract*—This paper quantifies the economic benefits of flexible Thermostatically Controlled Loads (TCLs) in a multi-area power system. The areas are connected via High Voltage Direct Current links. A distributed and non-disruptive control strategy manages the TCLs' operation to effectively schedule their consumption and, simultaneously, maintain headroom for several ancillary services. The TCLs' flexibility model is embedded in an optimal multi-area system scheduling model. The paper focuses on device-level metrics such as the annual cost savings obtained by single TCLs and compares these to system-level metrics e.g. system operation cost savings. Several case studies are built to assess key-drivers for TCLs' benefits.**

Keywords—Power system operation, Thermostatic loads, Unit commitment, Flexibility, HVDC

I. Introduction

Pursuant to environmental concerns, Renewable Energy Sources (RES) are contributing to phase conventional synchronous generators out of power networks [1]. However, RES-dominated power systems may suffer from the lack of inertial response. This would increase the risk of letting transient Rate of Change of Frequency (RoCoF) and/or maximum frequency deviation (nadir) drop below security thresholds unless significant amounts of ancillary services are rapidly delivered [2]. These issues are notably a concern for relatively small-medium networks such as in Ireland (IR) or Great Britain (GB) if compared to the size of the Continental Europe (CE) system. The level of interconnection between the power networks in IR, GB and CE has increased in the last years and this trend will be consolidated in the future [3]. Moreover, High Voltage Direct Current (HVDC) links are deployed to reach long distances through maritime borders. It is worth noting that each area of an HVDC-connected system is asynchronous with respect to the others, i.e. the frequency dynamics in one area are decoupled from those in others [4]. Hence, it becomes crucial to commit system assets to deliver, *locally*, sufficient fast frequency response services.

In the context of low-inertia, HVDC-connected power networks, there is growing interest in flexible, distributed resources, such as Thermostatically Controlled Loads. These appliances are relatively insensitive to small alterations to their regular operating cycle. The intrinsic TCLs' flexibility can be effectively exploited to simultaneously provide several short/medium term ancillary services, enable energy arbitrage and relieve possible congestions of HVDC links. In the last years, several works have investigated the TCLs' support to system needs focusing on technical and economic aspects (among others, [5]–[9]). Besides the fundamental contributions provided to the relevant literature, these works did not fully investigate the role and benefits of TCLs in multi-area and HVDC-connected power systems. This prevented from assessing the occurrence of potential synergies and/or conflicts with the flexible operation of HVDC links. Recently, a novel and relevant methodology has been developed [10]. It consists of a security-constrained System Scheduling Model (SSM) that optimally combines the *local* dimension of TCLs' flexibility with the *cross-border* dimension of the flexibility of HVDC interconnectors. The former is mainly exploited to ensure secure frequency transients in each area of the network, whereas the latter aims at enabling inter-area power flows. Up to different extent, the two layers of flexibility contribute to accommodate large shares of RES.

The work in [10] highlighted system-level interactions, suggesting a critical review of the typical operation of the HVDC links. Conversely, this paper takes the perspective of highlighting the role and the benefits of TCLs that provide a portfolio of ancillary services. The proposed methodology is applied to several case studies, which quantify the economic benefits of exploiting flexible TCLs under various system conditions, e.g., different RES penetrations and different shares of flexible TCLs within the cluster of devices. Moreover, other studies evaluate the sensitivity of the TCLs' economic benefits to devices' parameters and operating conditions. Finally, the impact of establishing alternative requirements for fast frequency response services is also evaluated; initial findings on the dependency of the TCLs' benefits on the geographical location are investigated.

II. Model Description

The schematics of the power system model adopted in this work is in Fig. 1. The three areas representing IR, GB and CE are connected via two HVDC links. This setup lets the frequency dynamics in one area be independent from those in the other areas. As in [10], the HVDC is assumed to not transfer cross-border frequency response services. Other system users considered are conventional synchronous generators (nuclear, Combined Cycle Gas Turbines – CCGT, and Open Cycle Gas Turbines – OCGT), RES represented by wind farms, inflexible load and flexible TCLs [7].

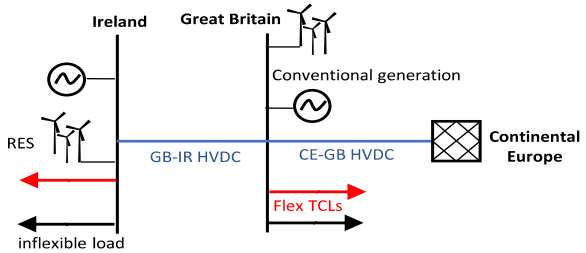

Fig. 1. Schematics of the multi-area, HVDC-connected power system.

The operation of the interconnected system is determined following a centralised approach. All the decisions variables (i.e., generation commitment/dispatch decisions, TCLs' operation, power flows through the HVDC links and the allocation of several ancillary services) are obtained by solving a single optimisation problem. The solution of this problem represents a lower bound for the aggregate operating costs of the power system in each area. The sizes of the three areas considered are quite different from each other. This

entails distinctive technical and economic issues in each area concerning the energy dispatch problem and, even more, the post-fault frequency control. The network in IR area is quite smaller than the one in GB, which, in turn, is significantly smaller than the size of the interconnected system in CE. It is therefore assumed that the CE scheduling is not explicitly modelled. The imported/exported flows of the CE-GB HVDC link would also depend on cost-quantity curves.

A. Contingency and Operational Ancillary Services

The allocation of the optimal amount of ancillary services to deal with unexpected events is pivotal in the scheduling of power systems. Two families of ancillary services are considered in this work: the *contingency ancillary services* and the *operational reserves* (ORs). The first group accounts for sudden infeed generation/load losses. In the aftermath of these events, frequency would rapidly drop/increase. During the transient, three conditions must be respected for both directions of frequency deviations: the *RoCoF*, the maximum frequency deviation (*nadir*) and the *quasi-steady state* frequency deviation must remain above specified thresholds. These conditions occur within a small interval (up to 30-60s) after the fault. The full recovery is performed over a larger time window 15-30 minutes, entailing slower dynamics.

The list of contingency ancillary services adopted in this work is in Table I. Besides intrinsic differences, natural inertia (NI), primary response (PR) and secondary response (SR) are rapidly delivered to deal with RoCoF, nadir and quasi-steady state conditions in the aftermath of a generation loss. The same objective is fulfilled by NI and high frequency response (HR) in the aftermath of a load loss. Upwards and downwards contingency reserves (CR_u and CR_d) guarantee the recovery to a pre-fault steady state condition, following a generation/load loss, respectively. The methodologies to compute the optimal system-level requirements of contingency ancillary services are presented in [10] and [11].

TABLE I. CHARACTERISTICS OF THE ANCILLARY SERVICES

Type			Characteristics	Providers
contingency ancillary services	Rapid delivery	NI	Use of kinetic energy in the rotating masses of synchronous units. Limited source that supports the RoCoF and nadir conditions.	All synchronous units
		PR	Automatic change in power output supplied by 5s (IR) 10s (GB) and sustained for 20s. It aids the RoCoF and the nadir conditions.	OGCT, CCGT, TCLs
		SR	Automatic change in power output supplied by 30s and sustained for tens of minutes. It aids the quasi-steady-state condition.	OGCT, CCGT, TCLs
		HR	Automatic change in power output. It combines PR and SR for positive deviations.	OGCT, CCGT, TCLs
	Slow delivery	CR_u	Long term power injection to recover the steady state. Provided by spinning or standing (to be brought on line) generators.	OGCT, CCGT (only spinning)
		CR_d	Spinning generators provide long term power reduction to recover the steady state after a positive frequency deviation.	OGCT, CCGT
operational Reserves		OR_u	Long term power injections to deal with a wind availability lower than expected.	OGCT, CCGT
		OR_d	Long term power reductions to deal with a wind availability higher than expected.	OGCT, CCGT

Furthermore, these requirements are computed against the maximum generation/load *local* outages in each area. This is in line with HVDC not providing cross-border ancillary services and the decoupled frequency dynamics of HVDC-connected areas. The second type of services handle with the intrinsic uncertainty characterising wind farms' outputs, to cope with power mismatches, upwards and downwards (Table I). Note that the power headroom dedicated to ORs cannot be overlapped with those for CRs, since the underlying events for which these reserves are scheduled are independent of each other, thus they may occur simultaneously. The system-level requirements for ORs depend on the expected wind availability. The relevant methodology is outlined in [10].

III. THERMOSTATICALLY CONTROLLED LOADS (TCLS)

The flexibility of a large cluster of individual heterogeneous TCLs indexed by u can be described by (1)-(4) as a single battery-like model with an evaporative term [12].

$$\dot{E}(\tau) = -(E(\tau)/\eta) + P(\tau) \quad (1)$$

$$P(\tau) = \Pi(\tau) \cdot P_0 + o\left(1/\sqrt{\tilde{N}}\right) \quad (2)$$

$$\min_u \underline{E}^{(u)} = \underline{E} \leq E(\tau) \leq \overline{E} = \min_u \overline{E}^{(u)} \quad (3)$$

$$\min_u \underline{P}^{(u)} = \underline{P} \leq P(\tau) \leq \overline{P} = \min_u \overline{P}^{(u)} \quad (4)$$

The aggregate energy and power levels are $E(\tau)$ [MWh] and $P(\tau)$ [MW], while η [h] is the time constant of the cluster model. The derivation of η from the time constants of single TCLs is shown in [12]. The underlying control strategy in [12] lets individual devices target the common desired relative power consumption $\Pi(\tau)$ such that (2) is ensured. Note that the steady-state aggregate consumption P_0 equals $\sum_u \left(\lambda^{(u)} \cdot P_{on}^{(u)}\right)$, with $\lambda^{(u)}$ being the duty cycle of a generic TCL and P_{on}^{u} [W] its power consumption when switched on. Moreover, since the devices are statistically independent of each other, $o(\cdot)$, the relative deviation of $P(\tau)$ from the target profile $\Pi(\tau) \cdot P_0$, decreases as $1/\sqrt{\tilde{N}}$ with $\tilde{N}$ the size of the cluster. Limitations on the thermal energy (3) prevent TCLs from operating outside permitted energy (i.e. temperature) ranges. Further restrictions (4) apply to the aggregate consumption. Any signal complying with (3)-(4) is feasible for single TCLs [12], ensuring satisfactory power tracking in (2).

A. Flexibility boundaries for aggregate TCLs.

Based on the properties described by (1)-(4) and the information in Table I, Fig. 2 illustrates the flexibility boundaries on the regular TCLs' energy/power consumption (black curves) and on the energy/power levels when delivering PR (initial drop of the dashed blue line), SR (dashed blue) and HR (dashed red), if these services are called upon.

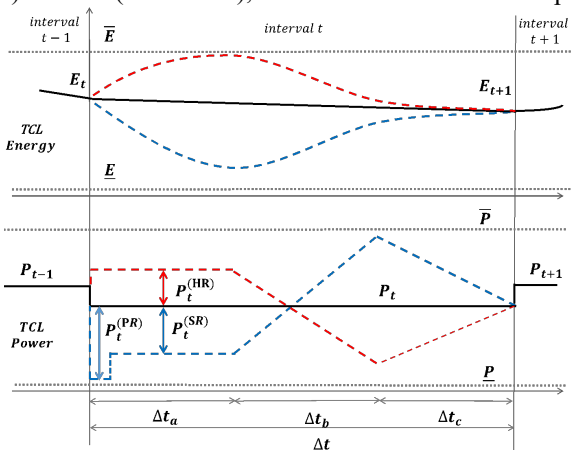

Fig. 2. Scheduling the regular TCL energy/power operation and allocation of contingency ancillary services.

At a generic interval t with duration Δt, the power level P_t reduces compared to P_{t-1}, forcing a reduction in the energy. Aggregate TCLs may decrease the consumption to deliver PR, $P_t^{(PR)}$ and SR, $P_t^{(SR)}$. This action determines a drop in the thermal energy across the time slot Δt_a. The energy

borrowed during this phase must be paid back by the end of the interval t. The recovery follows the path in Fig. 2 with peak above P_t, which depends on the amount of $P_t^{(\mathrm{SR})}$ and the duration of the time slots Δt_b and Δt_c, sub-intervals of Δt. The provision of HR ($P_t^{(\mathrm{HR})}$) entails an opposite behaviour.

Finally, certain feasible power/energy profiles could still affect the primary function of TCLs, causing the drift of the TCLs' aggregate energy over time. In other words, TCLs' energy may be kept at the upper/lower bounds for long periods (e.g., several hours). Hence, the mean value of the TCLs' calculated over energy over a certain time interval μ (left-hand side of (5)) must equal the steady state level $E_0 = \eta \cdot P_0$:

$$\frac{1}{\mu}\int_{\mu} E(\tau)d\tau = E_0. \tag{5}$$

IV. System Scheduling Model

This section recalls the main features of the multi-area system scheduling model (SSM) in [10] used in this work. The SSM is a deterministic, quadratic programming problem, where typical binary variables of generators are relaxed with continuous ones. For simplicity, the complete mathematical formulation of the SSM presented in [10] is not repeated below. However, Fig. 3 summarises the main characteristics of the objective function and all the constraints of the SSM. References to the corresponding equations in [10] are given. Details on the objective function and constraints on TCLs' flexibility are also recalled below. The horizon of the analysis is one year, with N=365 individual simulations. The time interval μ is set to 24 h (i.e. T=48 half-hourly intervals). The optimization horizon of each simulation is 48 h considering $2T$=96 steps of duration Δt=30 min each. According with a rolling-planning approach, the solution after the first 24 h is discarded. When moving from day n to $n+1$, relevant decisions variables and inter-temporal constraints are properly maintained. The SSM minimises the system operation costs:

$$\min_{\xi} \hat{F}(\xi) = \sum_{n=1}^{N}\Big\{\sum_{t=1}^{2T}\sum_{g\in\mathcal{G}}\Delta t\Big[c_g^{(\mathrm{nl})}\varphi_{g,t} + c_g^{(\mathrm{lp})}G_{g,t} + \\ + c_g^{(\mathrm{ql})}{G^2}_{g,t}\Delta t + c_g^{(\mathrm{su})}\chi_{g,t} + c_t^{(\mathrm{link})}P_t^{(\mathrm{link})}\Big]\Big\}_n \tag{6}$$

For all the generation technologies $g \in \mathcal{G}$, the first term is the product of the no-load (nl) cost and the fraction of generation technology g brought on line. The second and the third terms represent the production cost, a linear (lp) and quadratic (ql) function of the generation dispatch level $G_{g,t}$. The fourth term refers to the start-up (su) cost for the corresponding fraction of technology, $\chi_{g,t}$. The last term indicates the costs $c_t^{(\mathrm{link})}$ of the flow $P_t^{(\mathrm{link})}$ of the GB-CE link.

The schematics of the TCLs' flexibility in Fig. 2 are re-arranged as constraints (7)-(19) and embedded in the SSM.

$$\underline{E}_x \le E_{x,t} \le \overline{E}_x \tag{7}$$

$$\underline{P}_x \le P_{x,t} \le \overline{P}_x \tag{8}$$

$$0 \le P_{x,t}^{(\mathrm{PR})} \le P_{x,t} - \underline{P}_x \tag{9}$$

$$0 \le P_{x,t}^{(\mathrm{SR})} \le P_{x,t} - P_x \tag{10}$$

$$0 \le P_{x,t}^{(\mathrm{HR})} \le \overline{P}_x - P_{x,t} \tag{11}$$

$$P_{x,t} + \alpha_5 \cdot P_{x,t}^{(\mathrm{SR})} \le \overline{P}_x \tag{12}$$

$$P_{x,t} - \alpha_5 \cdot P_{x,t}^{(\mathrm{HR})} \ge \underline{P}_x \tag{13}$$

$$\alpha_3 \cdot E_{x,t} + \alpha_4 \cdot \left(P_{x,t} - P_{x,t}^{(\mathrm{SR})}\right) \ge \underline{E}_x \tag{14}$$

$$\alpha_6 \cdot E_{x,t} + \alpha_7 \cdot P_{x,t} + \alpha_8 \cdot P_{x,t}^{(\mathrm{SR})} \le \overline{E}_x \tag{15}$$

$$\alpha_3 \cdot E_{x,t} + \alpha_4 \cdot \left[P_{x,t} + P_{x,t}^{(\mathrm{HR})}\right] \le \overline{E}_x \tag{16}$$

$$\alpha_6 \cdot E_{x,t} + \alpha_7 \cdot P_{x,t} - \alpha_8 \cdot P_{x,t}^{(\mathrm{HR})} \ge \underline{E}_x \tag{17}$$

$$\frac{1}{T}[\alpha_9 \cdot E_{x,1} + \sum_{t=2}^{T} E_{x,t} + \alpha_{10} \cdot E_{x,(T+1)}] = E_{x,0} \tag{18}$$

$$\frac{1}{T}[\alpha_9 \cdot E_{x,(T+1)} + \sum_{t=T+2}^{T} E_{x,t} + \alpha_{10} \cdot E_{x,2T}] = E_{x,0} \tag{19}$$

For a generic interval t and area x, the thermal energies $E_{x,t}$ and $E_{x,t+1}$ are the actual decision variables and $P_{x,t}$ is explicated as $P_{x,t} = \left(E_{x,t+1} - \alpha_1 \cdot E_{x,t}\right)/\alpha_2$. The parameters α_1, α_2 and all the others in (12)-(18) are constant quantities that depend only on η and the lengths of Δt, Δt_a and Δt_b, as shown in [7] and [10]. The energy and power bounds in regular operation are set by (7)-(8), replicating (3)-(4) in a time-discrete formulation. As in Fig. 2, sufficient power headroom for PR, SR and HR are established by (9)-(11), respectively. Based on the actual allocation of SR or HR, (12) and (13) define the power increase (SR) or decrease (HR) reached at the end of Δt_b to perform the energy payback The components $\alpha_5 \cdot P_{x,t}^{(\mathrm{SR})}$ and $-\alpha_5 \cdot P_{x,t}^{(\mathrm{HR})}$ are integrated in the computation of the system-level requirements for the $\mathrm{CR_u}$ and $\mathrm{CR_d}$, [10]. The energy drop due to SR is bounded in (14). The energy level during the payback period after the delivery of SR is constrained in (15). The same aims are ensured by (16) and (17) in case of HR. The integral constraint (5) is implemented in a discrete environment by (18)-(19). Since optimization horizon in (6) is $2T$ intervals, two constraints are needed.

Objective: minimize generation production costs, start-up costs and Interconnectors costs (5) in [10].

Constraints on generation:
- *Feasibility*: (6)-(7) in [10]
- *Intertemporal*: ramping, min up and down, start up and shut down time (8)-(10), (13) in [10]
- *Headroom for ancillary services*: PR (11), SR (12), CR upwards (18), HR (37), CR downwards (38), OR upwards (39), OR downwards (40) in [10]
- *Energy – ancillary services dispatch:* (35)-(36), (42)-(43) in [10].

Constraints on TCLs:
- *Feasibility*: energy (20), power (21), PR (22), SR (23)-(24), HR (28)-(29), energy recovery (25)-(26), (30)-(31).
- *Daily energy management:* (27) in [10].

System-level constraints:
- *Power flows*: (14) in [10].
- *Ancillary services*: RoCoF (15a), (32a), PR (15b), SR (16), HR (32b)-(33), CR (17), (34), OR (41) in [10].

HVDC constraints:
- *Power flows*: (19), (44) in [10].

Continuity constraints:
- *Rolling planning*: (45) in [10].

Fig. 3. Summary of the SSM. Equations' numbers are referred to [10].

V. Case Studies

The values of input parameters of SSM in [10] are adopted for simulations. The installed capacities of conventional generation and their generation costs are repeated in Table II.

TABLE II. Conventional Generation – Main Quantities

Quantity	GB			IR	
	OCGT	CCGT	Nuclear	OCGT	CCGT
Capacity [GW]	28	32	9.6	3	5
Number of units N_g	90	40	6	10	6
$c_g^{(\mathrm{nl})}$ [k£/h]	$9\cdot N_g$	$8\cdot N_g$	$0.25\cdot N_g$	$9\cdot N_g$	$8\cdot N_g$
$c_g^{(\mathrm{lp})}$ [£/MWh]	110	45	5	110	45
$c_g^{(\mathrm{ql})}$ [£/(MWh)²]	0.015	0.005	0.005	0.02	0.01
$c_g^{(\mathrm{su})}$ [k£/h]	$1\cdot N_g$	$32\cdot N_g$	-	$1\cdot N_g$	$32\cdot N_g$

Figure 4a shows the duration curves of the wind availability in GB and IR. These quantities are in per unit of the relevant wind installed capacities, which vary among the case studies presented in Sec. V-A. The duration curves of the inflexible load in GB and IR are shown in Fig. 4b.

The domestic refrigerators in [10] are used in this work. Hence, the average rated power, duty cycle and time constant are $P_{on}^{(u)}$= 180W, $\lambda^{(u)}$= 0.218 and η= 5h, respectively. The TCLs' clusters in GB and IR are made of $\widetilde{N}_{GB}$=90 and $\widetilde{N}_{IR}$=18 million devices. At steady state, it results that $P_{GB,0}$ =

3.7GW, $P_{IR,0}$= 0.7GW, $E_{GB,0}$=16.8GWh and $E_{IR,0}$= 3.3 GWh. The numerical values of relevant parameters are in [10].

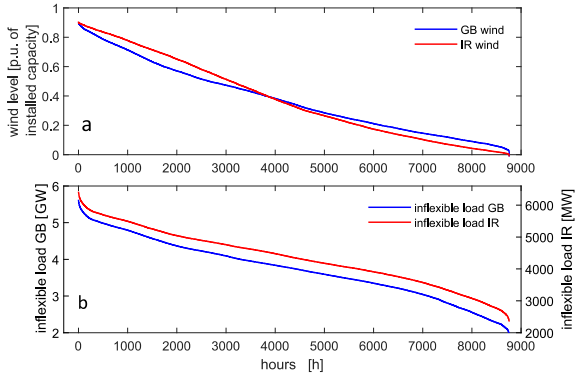

Fig. 4. a) duration curve of the wind availability expressed in p.u. of the relevant installed capacities; b) duration curve of the inflexible load.

A. Definition of the Case Study and Results

This paper aims at assessing the annual economic benefits for individual, flexible TCLs in the multi-area HVDC-connected power system in Fig.1. To improve the robustness of the results, nine case studies are presented in Fig. 5 to quantify the TCL's benefits over different conditions. Two leading factors characterise each case study. The first is the wind installed capacities in GB and IR; the second is the percentage of flexible TCLs in each area. The numbers identifying the case studies reflect the order of the elements of a 3x3 matrix. Hence, the CS_3_1 (dark grey square) suffers from the slowest progression towards a low-carbon paradigm. Only 10% of all the TCLs are flexible and the integration of wind generation is limited. Moving vertically from CS_3_1, the scenarios undertook *system transformations*, since the wind penetration grows with no increase in the shares of flexible TCLs. Instead, moving horizontally, low-carbon targets are fostered via *consumer transformations*. The share of flexible TCLs grows to 50% up to 100% (all TCLs are controlled as in Fig. 2), whereas the wind capacities are constant. Proceeding on the antidiagonal, the case-studies present more balanced transformation due to a mutual growth in wind capacities and in the shares of flexible TCLs. Finally, the most flexible and low-carbon scenario is therefore CS_1_3 (dark green square).

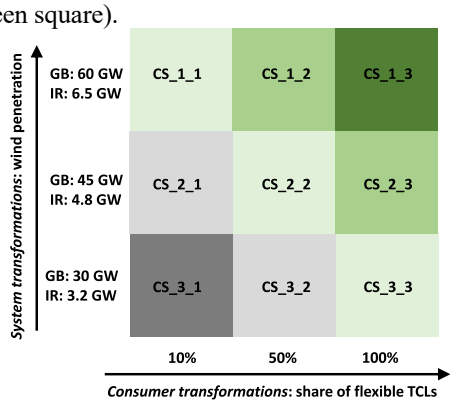

Fig. 5. Definition of the Case Studies.

The flexible allocation of several ancillary services let individual TCLs to realise the savings shown in Fig. 6. For each of the case studies defined by the indices $i \in \{1,2,3\}$ (rows) and $j \in \{1,2,3\}$ (columns), the savings $\beta_{i,j}^{(u)}$ of a generic appliance u in the subset of flexible TCLs $u \in \left\{1, \dots, \tilde{N}_{\mathrm{GB}}^{(\mathrm{flex})} + \tilde{N}_{\mathrm{GB}}^{(\mathrm{flex})}\right\} \subseteq \{1, \dots, \tilde{N}_{\mathrm{GB}} + \tilde{N}_{\mathrm{IR}}\}$ are computed as:

$$\beta_{i,j}^{(u)} = \left(F_{i,j} - F_{i,j}^{0}\right) / \left(\tilde{N}_{\mathrm{GB}}^{(\mathrm{flex})} + \tilde{N}_{\mathrm{GB}}^{(\mathrm{flex})}\right). \quad (20)$$

Note that $F_{i,j}$ is the total system operation cost sustained in the case study (i,j), whereas $F_{i,j}^{0}$ is the same quantity if all TCLs were inflexible i.e. $P_{x,t} = P_{x,0}$, $E_{x,t} = E_{x,0}$, $P_{x,t}^{(\mathrm{PR})} = P_{x,t}^{(\mathrm{SR})} = P_{x,t}^{(\mathrm{HR})} = 0$ at all times and for $x \in \{\mathrm{GB}, \mathrm{IR}\}$.

Results demonstrate that increasing the wind penetrations (i.e. from the rightmost to the leftmost sets of bars in Fig. 6) enables larger savings for individual TCLs. This trend occurs for the three shares of flexible TCLs (the columns in Fig. 5). On the other hand, when fixing the wind penetration (one of the three sets of bars in Fig. 6), higher savings are achieved for low penetrations (10%) of flexible TCLs (first column of the matrix in Fig. 5). This may represent a strong incentive for entities like aggregators or individual customers to start and spread the implementation of flexible TCLs for demand response actions. A saturation effect for increasing levels of wind can be noted. Considering, for instance, 50% of flexible TCLs, an increase of 16.6 GW in the total wind capacity (from row 3 to row 2 in Fig. 5) triggers a boost of 41-28.3=12.7£ in the TCLs' savings. The same increase in wind capacity, when moving from the values in row 2 to row 1 in Fig. 5, determine a boost of 49-41=8£ in the corresponding TCLs' savings.

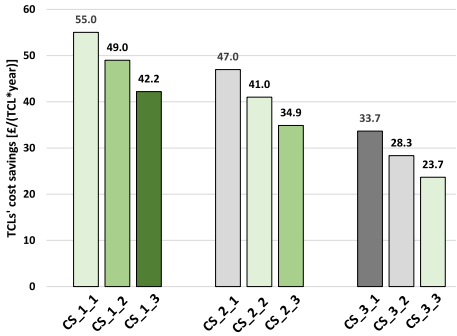

Fig. 6. Annual TCL cost savings for all the simulated case studies in Fig. 5.

Figure 7 outlines system-level trends and it illustrates the percent reductions $\beta_{i,j}^{\%}$ in the system operation costs for the case studies in Fig. 5. In accordance with (20), these are computed as $\beta_{i,j}^{\%} = -100 \cdot \left(F_{i,j} - F_{i,j}^{0}\right) / F_{i,j}^{0}$. The trends described in Fig. 6 are partially inverted here. For all the wind conditions, higher cost savings are achieved when all the TCLs are flexible (100%). Hence, the benefits for the system operator or the "social value" of demand response increase with more *consumer transformations* implemented. As in Fig. 6, the largest savings occur for high wind conditions.

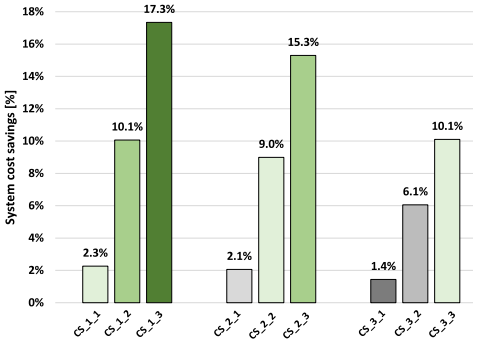

Fig. 7. System cost savings for all the simulated case studies in Fig. 5.

Keeping the focus on system-level outcomes, Table III reports the annual wind curtailment percent index $\mathcal{C}_{i,j}^{\%}$ for all the case studies in Fig. 5. It is computed as in (22) and is the weighted average of the curtailment indices in GB and IR, where the weights are the installed wind capacities $\bar{G}_{i,x}^{(\mathrm{wind})}$ for each row $i \in \{1,2,3\}$ of the matrix in Fig. 5 and in each area

$x \in \{\text{GB}, \text{IR}\}$. Note that $\check{G}_{i,j}^{(\text{wind})}$ represents the wind generation at each time step t actually dispatched (i.e. the solution of the underlying optimal SSM). Finally, $\hat{G}_i^{(\text{wind})}$ is the available wind at the corresponding time step.

$$C_{i,j}^{\%} = \frac{\sum_{x\in\{\text{GB,IR}\}} \left[\sum_{\substack{n\in\{1\dots N\} \\ t\in\{1\dots T\}}} \left(\frac{\check{G}_{i,j}^{(\text{wind})} - \hat{G}_i^{(\text{wind})}}{\hat{G}_i^{(\text{wind})}} \right)_{t,n} \cdot \bar{G}_i^{(\text{wind})} \right]_x}{\bar{G}_{i,GB}^{(\text{wind})} + \bar{G}_{i,IR}^{(\text{wind})}} \tag{22}$$

Higher shares of flexible TCLs (moving from column 1 to column 3) reduce the wind curtailment indices. Note that, in low wind conditions (row 3), most of the available wind can be integrated ($C_{3,j}^{\%} \leq 1\%$) mainly due to the large amount of committed NI from synchronous units.

TABLE III. WIND CURTAILMENT AS PERCENTAGE OF AVAILABLE WIND

Assumption on installed wind	Assumption on the penetration of flexible TCLs		
	Column 1	Column 2	Column 3
Row 1	15.5 %	13.4 %	11.3 %
Row 2	7.1 %	5.5 %	3.8 %
Row 3	1.0 %	0.6 %	0.2 %

B. *Sensititvity to parameters of TCLs*

This section deals with the sensitivity of the individual TCLs' annual cost savings to certain TCLs-related conditions and parameters. The analysis is carried out taking CS_2_2 in Fig. 5 as reference. All the arising trends can be extended to other case studies. The installed wind capacities in GB and IR are 45 GW and 4.8 GW, respectively. The shares of flexible TCLs are 50% of the entire clusters in each area.

Results in Fig. 8 show the impact of increasing the coefficient of performance (CoP) of TCLs (CoP=3 in the reference case). The CoP is defined as the ratio of the heat extracted from the refrigerating compartment over the electrical energy absorbed to perform the action [13]. The CoP is an indicator of the efficiency of the TCL. Changes to the CoP entail variations to the main parameters of the TCLs' thermal model (1)-(4). Overall, the economic benefits for single TCLs reduce for higher CoPs. Two reasons contribute to this decrement and are characterized by opposite trends. On the one hand, more efficient TCLs require, on average, lower consumptions. This allows for *energy savings* (orange bars), which actually increase for higher values of CoP. On the other hand, lower consumptions reduce the relative power/energy TCLs' support in the fulfilment of system-level requirements for ancillary services (blue bars decrease).

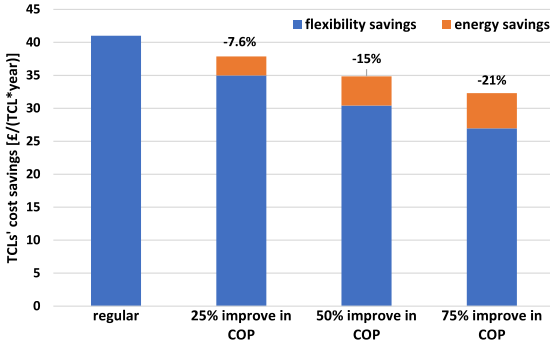

Fig. 8. Annual TCLs' cost savings for varying the CoP of the devices.

The integral constraints (18)-(19) ensure that the TCLs' average thermal energy (i.e. temperature) is properly maintained over time. However, a flexible operation would still require periods of time during which TCLs reach the upper/lower energy bounds (lower/upper temperatures), possibly affecting their primary cooling function. This may happen in regular operation (based on (8)) or during the rare actual provisions of ancillary services (e.g. (12), (14)-(17)). The results in Fig. 9 illustrate the percent variation in TCLs' cost savings (with respect to the reference CS_2_2 when the thermal energy buffer $\overline{E}_x - \underline{E}_x$ is reduced but still centred on $E_{x,0}$. Starting from the reference values of the energy thresholds $\overline{E}_x, \underline{E}_x$, the new energy thresholds $\overline{E}_x^{'}, \underline{E}_x^{'}$ after the application of a reducing factor $r \in [0,1]$ are

$$\begin{aligned} \overline{E}_x^{'} &= \underline{E}_x^{'} + (1-r)\cdot\left(\overline{E}_x - \underline{E}_x\right) \\ \underline{E}_x^{'} &= \overline{E}_x + \underline{E}_x - \overline{E}_x^{'} \end{aligned} \tag{23}$$

where the second equation maintains the same central value at the midpoint of the threshold range.

The first two bars from the top in Fig. 9 impose 10% and 20% reductions, respectively, to the energy thresholds, both in regular operation (for energy arbitrage purposes) and in the allocation of ancillary services. The third and fourth bars apply the reductions only during the regular operation. The underlying motivation is that the actual delivery of ancillary services is rare thus, during those events, the TCLs' energy (temperatures) may hit $\overline{E}_x, \underline{E}_x$ without causing much discomfort. The bottom bar refers to the reference case with no reductions. Considering the third and fourth bars, it is clear the TCLs' economic benefits are limited by bounds on the power excursions rather than by constraints on the energy buffer. Only small reductions in the cost savings are reported.

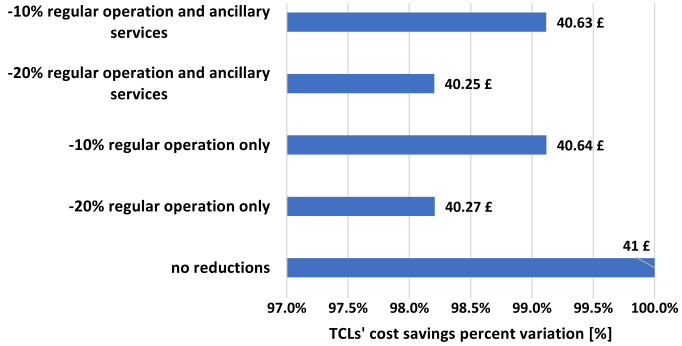

Fig. 9. Percent variations in the TCLs' cost savings varying the thermal energy thresholds for regular operation and/or delivery of ancillary services.

Furthermore, the additional drop in the TCL's savings, when the reduction in the energy thresholds is extended to the provision of ancillary services (first two bars), is almost negligible. This further confirms that the system requires more *power-flexibility* rather than *energy-flexibility*. In fact, TCLs are do not noticeably reduce their economic benefits when power-intensive ancillary services e.g. PR are fully enabled, whereas energy-intensive ones such as SR are limited due to reductions in the overall energy buffer (first two bars). Note that similar studies, assessing the impact of reductions in the power buffer $\overline{P}_x - \underline{P}_x$, have not been carried out since these are part of the design of the control strategy in [12]. In fact, changes to the power buffer do not affect the primary cooling function of refrigerators. In this case, there would be no incentive for consumers to reduce it.

C. *Sensitivity to system-level conditions*

This section explores the sensitivity of the TCLs' cost savings to changes to system-level conditions. Once again, the CS_2_2 in Fig. 5 is the reference case. The first study, whose results are in Fig. 10, investigates the impact of reducing the delivery time of PR and HR from 10 s as in the reference down to 5 s (note that 5 s was already adopted in IR in the reference case). This potential change to the structure of fast frequency

response services is expected to boost the role of conventional generators in the fulfilment of system-level requirements. Conventional units would shorten the spread between their dynamic capabilities and those of TCLs. The total amount of frequency response services would ultimately reduce. Hence, Fig. 10 indicates a reduction in the TCLs' cost savings by more than 25% (blue bars). As expected, the system operation costs also decline (orange dots).

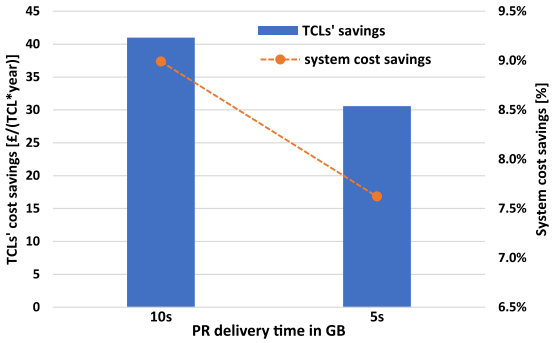

Fig. 10. Annual TCLs' cost savings (bars) and system operation cost savings (dots) varying the delivery time of PR and HR in GB.

Finally, three additional scenarios are derived from the reference case and compared to it. The main characteristics are in the share and location of flexible TCLs. In particular:

i. 50% of flexible TCLs in GB ($\tilde{N}_{GB}^{flex}$= 45 Mil.), 0% in IR.
ii. 0% in GB, 50% of flexible TCLs in IR ($\tilde{N}_{IR}^{flex}$= 9 Mil.).
iii. 10% of flexible TCLs in GB ($\tilde{N}_{GB}^{flex}$= 9 Mil.), 0% in IR.

Note that the cases i. and ii. have in common the same share of flexible TCLs (50%) but at different areas. The cases ii. and iii. instead have in common the same number of flexible TCLs (9 Mil.), again at different areas. The outcomes of the three studies are reported in Fig. 11 and compared to those of the reference case. The largest economic benefits are for TCLs under the assumptions of case ii., potentially suggesting that, from the perspective of a single device, the TCLs' flexibility in IR is more beneficial than in GB. This overall result is not only driven by the fact that a smaller number of flexible TCLs (i.e. case ii. vs. case i.) brings higher benefits, as in Fig. 6. In fact, the outcomes of case iii. show that the same number of flexible TCLs as in case ii. (9 Mil.) would collect almost 27 £ less if they were located in GB rather than in IR. It is worth noting that the TCLs' cost savings in case iii. are equivalent to those of the reference case.

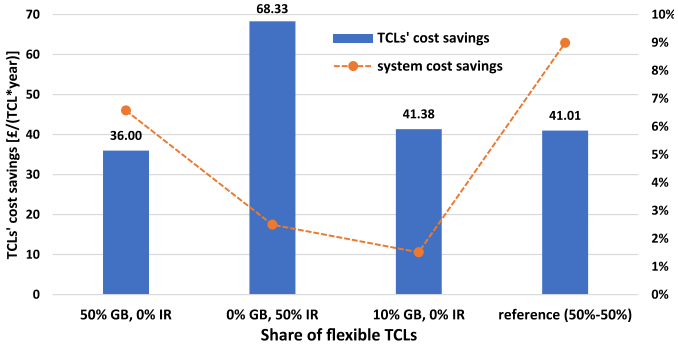

Fig. 11. Annual TCLs' cost savings (bars) and system operation cost savings (dots) for different shares of TCLs' flexibility allowed only in one area.

The resulting trends concerning the percent variations in system operation costs validate the analysis above and previous results. First, 9 Mil. of flexible TCLs in GB (case iii.) enable a system cost reduction (1.5%) lower than if the same number of smart devices were located in IR (2.5 % - case ii.). Second, in line with the trends in Fig. 7, the larger the pool of flexible devices, the higher the contribution for the system. The percent system cost savings for the reference case is 9% with 54 Mil. flexible devices, which is significantly larger than those obtained in the other cases with fewer flexible TCLs (45 Mil. in case i. and 9. Mil. in cases ii. and iii.).

VI. Conclusions

This paper builds on a novel methodology for optimal scheduling of multi-area power systems connected by HVDC links [10]. This methodology has been successfully applied to several case studies that assess the economic benefits for individual TCLs located at different areas of the interconnected system. Under a large number of simulated conditions, results proved the possibility for individual TCLs to obtain significant cost savings if controlled as in Sec. III to provide several ancillary services. Three main challenges are yet to be overcome towards a full TCLs' contribution to system flexibility needs. First, the proposed cost-based approach should be extended to develop a detailed business model that recognizes the TCLs' role into a market-based framework. Second, a robust methodology to manage the uncertainty on TCLs' parameters is pivotal in case of large clusters including different classes of TCLs. Third, it is necessary to complement the economic-financial analysis on TCLs with a detailed study on the infrastructure(s) in charge of measuring, transferring and managing all relevant TCLs' data (e.g. included in the wider concept of the Internet of Things). These issues are part of the authors' ongoing work.

References

[1] National Grid, "Future Energy Scenarios," 2020. [Online]. Available: https://www.nationalgrideso.com/future-energy

[2] S.C. Johnson, J.D. Rhodes, M.E. Webber, "Understanding the impact of non-synchronous wind and solar generation ongrid stability and identifying mitigation pathways," *Applied Energy,* vol. 262, 2020.

[3] Ofgem, "Electricity Interconnectors," [Online]. Available: https://www.ofgem.gov. uk/electricity/transmission-networks/electricity-interconnectors.

[4] A. Tosatto, T. Weckesser, S. Chatzivasileiadis, "Market Integration of HVDC Lines: Internalizing HVDC Losses in Market Clearing," *IEEE Trans. Power Syst.,* vol. 35, no. 1, pp. 451-461, 2020.

[5] V. Trovato, S. Tindemans, G. Strbac, "Designing effective frequency response patterns for flexible thermostatic loads," in *15th IEEE EEEIC*, 2015.

[6] Y. Ding et al., "Multi-state oeprating reserve model for aggregate thermostatically controlled loads for power system short term reliability evaluation," *Applied Energy,* vol. 241, pp. 45-68, 2019.

[7] V. Trovato, F. Teng, G. Strbac, "Value of Thermostatic Loads in Future Low-Carbon Great Britain System," in *19th IEEE PSCC*, 2016.

[8] M. Zhang, et al., "Stochastic unit commitment with air conditioning loads participating in reserve service," *IET Renew. Power Generation,* vol. 13, no. 16, 2019.

[9] F. Teng, M. Aunedi, G. Strbac, V. Trovato, A. Dallagi, "Provision of ancillary services in future low-carbon UK electricity system," in *IEEE PES ISGT Conference*, 2017.

[10] V. Trovato, A. Mazza, G. Chicco, "Flexible operation of low-inertia power systems connected via high voltage direct current," *Electric Power System Research,* vol. 192, no. 106911, 2021.

[11] F. Teng, V. Trovato, G. Strbac, "Stochastic Scheduling With Inertia-Dependent Fast Frequency Response Requirements," *IEEE Trans. Power Syst.,* vol. 31, no. 2, pp. 1557 - 1566, 2016.

[12] V. Trovato, S. Tindemans, G. Strbac, "Leaky storage model for optimal multi-service allocation of thermostatic loads," *IET Generation, Transmission & Distribution,* vol. 10, no. 3, 2016.

[13] R. D. Knight, "Heat Engines and Refrigerators," in *Physics for Scientists and Engineers: A Strategic Approach*, San Francisco, Pearson Addison-Wesley, 2008.